Monthly Notices
of the
ROYAL ASTRONOMICAL SOCIETY

Mon. Not. R. Astron. Soc. **414,** 3645–3655 (2011) doi:10.1111/j.1365-2966.2011.18665.x

Large-scale nested stellar discs in NGC 7217★

Olga K. Sil'chenko,[1,2]† Igor V. Chilingarian,[1,3] Natalia Ya. Sotnikova[4,5]† and Victor L. Afanasiev[6]

[1]*Sternberg Astronomical Institute, Moscow State University, 13 Universitetski prospect, 119992 Moscow, Russia*
[2]*Isaac Newton Institute of Chile, Moscow Branch*
[3]*Centre de Données astronomiques de Strasbourg – Observatoire de Strasbourg, CNRS UMR 7550, Université de Strasbourg, 11 Rue de l'Université, 67000 Strasbourg, France*
[4]*St. Petersburg State University 7-9, Universitetskaya nab., St. Petersburg 199034, Russia*
[5]*Isaac Newton Institute of Chile, St. Petersburg Branch*
[6]*Special Astrophysical Observatory, Russian Academy of Sciences, Nizhnij Arkhyz, Russia*

Accepted 2011 March 7. Received 2011 March 2; in original form 2010 November 4

ABSTRACT

NGC 7217 is an unbarred early-type spiral galaxy having a multisegment exponential light profile and a system of star-forming rings of the unknown origin; it also possesses a circumnuclear gaseous polar disc. We analysed new long-slit spectroscopic data for NGC 7217 and derived the radial distributions of its stellar population parameters, and stellar and gaseous kinematics up to the radius of $r \approx 100$ arcsec ($\sim$8 kpc). We performed the dynamical analysis of the galaxy by recovering its velocity ellipsoid at different radii and estimated the scale-heights of its two exponential discs. The inner exponential stellar disc of NGC 7217 appears to be thin and harbours intermediate-age stars ($t_{\rm SSP} \approx 5$ Gyr). The outer stellar disc seen between the radii of 4 and 7 kpc is very thick ($z_0 = 1, \ldots, 3$ kpc), metal-poor, [Fe/H] < -0.4 dex, and has predominantly young stars, $t_{\rm SSP} = 2$ Gyr. The remnants of minor mergers of gas-rich satellites with an early-type giant disc galaxy available in the GalMer data base well resemble different structural components of NGC 7217, suggesting two minor merger events in the past responsible for the formation of the inner polar gaseous disc and large outer star-forming ring. Another possibility to form the outer ring is the re-accretion of the tidal streams created by the first minor merger.

Key words: galaxies: evolution – galaxies: individual: NGC 7217 – galaxies: spiral – galaxies: structure.

1 INTRODUCTION

Currently, our views on the galaxy structure are changing dramatically. The classical view that every disc galaxy represents a combination of a de Vaucouleurs bulge, a sort of an elliptical galaxy inside a larger stellar system and an exponential large-scale stellar disc (e.g. Freeman 1970) does not conform to modern high-accuracy observations, in particular to photometric data. With the surface photometry reaching low surface brightness limits, down to 27–28 mag arcsec^{-2} in the r band, the brightness profiles of most large-scale stellar discs cannot be fitted by a single-component exponential law: 90 per cent of discs turn to be either truncated or antitruncated (Pohlen & Trujillo 2006). Bulges also appear to be far from de Vaucouleurs' spheroids: when approximated by a Sérsic law with a free power parameter, they show surface brightness profile shapes spanning a range of n, with the mean $n \approx 2$ (Andredakis, Peletier & Balcells 1995; Seigar & James 1998; Graham 2001; Mollenhoff & Heidt 2001). Some morphological types, namely spirals later than Sbc (Andredakis & Sanders 1994) and lenticulars (Balcells et al. 2003; Laurikainen, Salo & Buta 2005), exhibit exponential surface brightness profiles for their bulges. The scatter in the concentration parameter n is thought to be related to a variety of bulge formation mechanisms; a range of scenarios is also restricted by dynamical properties of the bulges of different types.

Currently, all bulges are divided into two categories: 'classical' high-luminosity bulges which are suggested to be formed by fast violent events like mergers and 'pseudo-bulges'. The bulges of the latter type promulgated by J. Kormendy (see Kormendy 1993 and earlier conference contributions) are thought to form by the secular evolution from the gaseous and stellar material of the disc (Kormendy & Kennicutt 2004), in particular through the central disc heating by bars (Combes & Sanders 1981); hence, they have to resemble discs by some of their dynamical characteristics. Balcells, Graham & Peletier (2007) noted the presence of a lot of separate

★Based on the observations with the Russian 6-m telescope.
†E-mail: olga@sai.msu.su (OKS); nsot-astro@mail.ru (NYS)

discy stellar structures in the centres of spiral galaxies and Erwin et al. (2003) demonstrated that sometimes inner discs in early-type disc galaxies might resemble bulges. Although, following this fashion, a great variety of central structures often found in early-type disc galaxies (see e.g. Erwin & Sparke 2002) are now treated as the pseudo-bulges including nuclear discs and bars (Drory & Fisher 2007), we would like to stay on the classical point of view that the principal difference between discs and bulges is related to their thickness: discs are thin, flat, roughly two-dimensional structures and bulges must be thick and three-dimensional by definition. Pseudo-bulges being produced by secular-evolution mechanisms may have exponential surface brightness profiles (Friedli & Benz 1995), but they differ principally from the exponential stellar discs in their thickness. To put a quantitative criterion to distinguish between discs and spheroids, let us take a look on the phenomenology. E. Hubble classified elliptical galaxies by their shape ranging between *E0* (the axial ratio of 1) and *E7* (the axial ratio of 3); however, many former *E7* galaxies are now thought to be lenticulars, NGC 3115 being a famous example. As for the large-scale stellar discs, the closest axial ratio to the transition towards spheroids is perhaps demonstrated by the thick disc of the edge-on spiral galaxy NGC 891: its ratio of the exponential scalelength to the exponential scaleheight is about 3.3 (Ibata, Mouhcine & Rejkuba 2009). Hence, we consider that the ratio of the scalelength to scaleheight of about 3 is a reasonable frontier between spheroids and discs.

While analysing a photometric structure of a disc galaxy inclined to the line of sight, we can trace the ellipticity of its isophotes to establish a transition radius where the thick central structure, the bulge, delegates a dominance to the thin disc: it is the radius where the isophote ellipticity stops raising. For a galaxy at a small inclination, it is very difficult to distinguish between its exponential pseudo-bulge and a disc without a three-dimensional dynamical model of a galaxy. We attempted to construct such a model for the galaxy NGC 7217, for which there is still no agreement on the structure and origin of its inner subsystems.

NGC 7217 is a giant early-type spiral galaxy seen almost face-on. The distance to the galaxy adopted in our paper, 18.4 Mpc, was estimated from the Tully–Fisher relation by Russell (2002). It corresponds to the spatial scale of 0.08 kpc arcsec^{-1}. NGC 7217 is listed in the catalogue of isolated galaxies by Karachentseva (1973); in a more recent study by Bettoni, Galletta & Prada (2001), the density of its environment is also estimated as zero. The galaxy whose evolution is supposedly free of the environmental influence demonstrates a set of enigmatic structures which can be best explained by (a set of) minor mergers. First of all, it has three star-forming rings, at the radii of 11, 33 and 75 arcsec (Buta & Crocker 1993), looking like resonance structures requiring the presence of a non-axisymmetric potential (Verdes-Montenegro, Bosma & Athanassoula 1995), while the galaxy itself is unbarred. Buta et al. (1995) proposed to decompose the whole galaxy into a small disc and a large mildly triaxial de Vaucouleurs spheroid dominating at all distances from the centre. The dominance of the bulge triaxial potential over the whole galaxy caused the formation of three resonance rings with high-density gas concentration and ongoing star formation. Later, we undertook our own decomposition of the NGC 7217 structure and have found two large exponential components with different scalelengths[1]: 12.5 arcsec or 1 kpc for the inner one and 35.8 arcsec or about 3 kpc for the outer one (Sil'chenko & Afanasiev 2000). The inner component has larger intrinsic ellipticity than the outer one and so may be oval, providing the necessary triaxiality of the potential to put the rings at the resonance radii. The bulge, if any, is small, confined to the innermost (nuclear) ring and exponential. To choose between the alternate ways of decomposition, the kinematical data and a dynamical model are needed. The situation is complicated by the fresh (?) remnants of a minor merger presented by counter-rotating stars in the inner disc (Merrifield & Kuijken 1994) and the inner gas polar disc within $R \approx 4$ arcsec (Sil'chenko & Afanasiev 2000).

In this paper, we present the results of the long-slit spectroscopy of NGC 7217. Our goal is the diagnostics of the nature of the two large-scale exponential structures in this galaxy. The inner exponential structure may be an inner disc (a thin structure) or a pseudo-bulge (a thick structure). Since NGC 7217 is seen nearly face-on, the isophote ellipticity is a poor indicator of the stellar component thickness as it is close to zero over the whole galaxy. However, with the stellar velocity dispersion profiles along the major-axis and minor-axis, we can try to estimate the scaleheights of the stellar components from dynamical considerations. In Section 2, we describe our observations, data reduction and analysis and in Section 3 we provide our new estimates of the stellar population properties at different radii. Principal Section 4 gives our dynamical consideration of the NGC 7217 large-scale structures and Section 5 contains a discussion about the origin of the galaxy structure including the comparison with numerical simulations. In Section 6, we give a brief summary of our results.

2 OBSERVATIONS AND DATA REDUCTION

The spectroscopic observations were carried out with the SCORPIO[2] universal spectrograph (Afanasiev & Moiseev 2005) installed at the prime focus of the Russian 6-m Bol'shoy Teleskop Azimutal'nyy operated by the Special Astrophysical Observatory, Russian Academy of Sciences. We used the *VPHG*2300*G* grating providing an intermediate spectral resolution ($R \approx 2200$) in a relatively narrow wavelength region ($4800 < \lambda < 5500$ Å); however, it contains a rich set of strong absorption-line features, making it suitable for studying both internal kinematics and stellar populations of a galaxy. The chosen spectral range also includes several emission lines, Hβ, [O III] and [N I], which we used to derive the gas kinematics and line ratios. The slit was 1.0 arcsec wide and 6 arcmin long. The 2k × 2k EEV CCD42-40 detector used in the 1 × 2 binning mode provided a spectral sampling of 0.37 Å pixel^{-1} and a spatial scale of 0.357 arcsec pixel^{-1}.

We observed NGC 7217 in two slit positions going through the centre, along the minor-axis and major-axis of its inner isophotes. The major-axis spectrum, PA = 81°, where PA denotes the position angle, was obtained on 2008 October 6 with an integration time of 80 min under atmosphere conditions with good transparency and the intermediate image quality of 1.7 arcsec full width at half-maximum corresponding to the median seeing at the telescope site. The minor-axis data at PA = 169° were collected during two nights 2008 October 6 and October 8 with a total exposure time of 75 min under bad variable transparency and the seeing quality of ∼3 arcsec, making them notably shallower than the major-axis spectra. We obtained the following calibrations: night-time internal flat-field

[1] The bulge also demonstrates an exponential profile with a scalelength ∼4 arcsec (Sil'chenko & Afanasiev 2000).

[2] For a description of the SCORPIO instrument, see http://www.sao.ru/hq/moisav/scorpio/scorpio.html

and arc-line spectra, the GD 248 spectrophotometric standard star and high signal-to-noise ratio twilight spectral frames.

The data reduction and analysis for the spectral data of NGC 7217 were identical to that of the lenticular galaxy NGC 6340 presented in Chilingarian et al. (2009). We refer to that paper for all details; here, we give only essential information required for understanding our data analysis and interpretation.

The primary data-reduction steps included bias subtraction, flat-fielding and cosmic-ray hit removal using the Laplacian filtering technique (van Dokkum 2001). Then, we built the wavelength solution by identifying arc lines and fitting their positions using a third-order two-dimensional polynomial along and across dispersion, and linearized the spectra. The obtained wavelength solution had fitting residuals of about 0.08 Å rms.

The SCORPIO spectrograph has significant variations in the spectral line spread function (LSF) along and across the wavelength direction (see Moiseev 2008 and Chilingarian et al. 2009 for details). In our observations of NGC 7217, we used the peripheral regions of the slit beyond 2 arcmin from the galaxy centre to estimate the night-sky spectrum; therefore, it was very important to take the LSF variations into account in order to minimize the effects of the sky-subtraction artefacts on the data analysis. We mapped the LSF by fitting the high-resolution ($R = 10\,000$) solar spectrum against the twilight spectra at 64 positions along the slit in five slightly overlapping wavelength segments covering the spectral range of the SCORPIO setup with the penalized pixel-fitting technique (Cappellari & Emsellem 2004). We used the Gauss–Hermite parametrization up to the fourth order (van der Marel & Franx 1993) to represent the LSF shape.

Then, we modelled the night-sky spectrum at every position along the slit, following the procedure described in detail in Chilingarian et al. (2009) where the main step was the parametric signal recovery applied to the sky spectrum taken in the outer regions of the slit in the Fourier space as follows:

$$f(x,\lambda) = F^{-1}(F(f(\mathrm{sky},\lambda))\frac{F(\mathcal{L}(x))}{F(\mathcal{L}(\mathrm{sky}))}), \quad (1)$$

where $f(x, \lambda)$ denotes a sky spectrum at the position x along the slit with its parametrized LSF $\mathcal{L}(x)$; $f(\mathrm{sky}, \lambda)$ is the night-sky spectrum in any region of the slit with the LSF $\mathcal{L}(\mathrm{sky})$, and F and F^{-1} are the direct and inverse Fourier transforms, respectively. The night-sky model created in this fashion results in a nearly Poisson quality of the sky subtraction which is absolutely crucial for our analysis of the external regions of the galaxy.

3 STELLAR POPULATIONS AND INTERNAL KINEMATICS OF NGC 7217

We derived the parameters of internal kinematics and stellar populations of NGC 7217 by fitting high-resolution PEGASE.HR (Le Borgne et al. 2004) simple stellar population (SSP) models against our spectra with the NBURSTS full spectral fitting technique (Chilingarian et al. 2007a,b). The SSP models were computed using the Salpeter (1955) stellar initial mass function. The fitting algorithm is picking up a template from a grid of stellar population models in the age–metallicity space convolved with the instrumental response of the spectrograph (see previous section), broadening it with the line-of-sight velocity distribution (LOSVD) of a galaxy represented by the Gauss–Hermite parametrization up to the fourth order, that is, v, σ, h_3 and h_4. The models are multiplied pixel by pixel by the nth-order Legendre polynomial continuum which is used to account for possible imperfections of the flux calibration and for the internal dust extinction in a galaxy. All kinematical and stellar population parameters are determined in a single non-linear minimization loop, therefore reducing possible degeneracies. χ^2 is penalized towards a purely Gaussian LOSVD as explained in Cappellari & Emsellem (2004) in order to stabilize the solution in the case of low signal-to-noise ratios and/or insufficient spectral sampling of the data. We stress that for the dynamical analysis presented below, we use the pure Gaussian LOSVD parametrization without χ^2 penalization.

The PEGASE.HR models are constructed from empirical stellar spectra in the solar neighbourhood where the values of α-element abundances are known to correlate with the overall metallicity. Therefore, at intermediate and high metallicities, our SSP models are representative of the solar α/Fe abundance ratio. However, Chilingarian et al. (2008) showed that supersolar α/Fe ratios bias neither age nor metallicity estimates when using the NBURSTS spectral fitting technique and Sil'chenko & Afanasiev (2000) found nearly solar α/Fe in NGC 7217.

NGC 7217 possesses quite strong emission lines in its spectrum, especially in the regions corresponding to the rings with ongoing star formation. Therefore, we had to exclude from the fitting procedure several narrow 20-Å-wide regions around emission lines (Hβ λ = 4861 Å, [O III] λ = 4959, 5007 Å and [N I] λ = 5197, 5201 Å) redshifted according to the line-of-sight velocity of NGC 7217. Chilingarian (2009) demonstrated that Hβ contains 20 per cent of the age-sensitive information at the maximum when using the NBURSTS technique in a spectral range similar to ours; therefore, excluding it from the fit neither biases age estimates (see also appendix A2 in Chilingarian et al. 2007b and appendix B in Chilingarian et al. 2008) nor degrades significantly the quality of the age determination.

We fitted Gaussians pre-convolved with the SCORPIO LSF into the [O III] and Hβ emission lines in the residuals of the stellar population fitting and determined the ionized gas kinematics independently in the two lines as well as the emission-line flux ratios.

The obtained radial distributions of the SSP-equivalent age and metallicity of NGC 7217 are shown in Fig. 1. Sil'chenko & Afanasiev (2000) analysed the large-scale structure of NGC 7217 and identified three galaxy components: a bulge dominating at radii 5–15 arcsec (0.4–1.2 kpc) and two exponential structures interpreted as discs. The inner and outer discs dominate in the galaxy light profile at 20–50 arcsec (1.6–4 kpc) and 60–110 arcsec (4.8–8.8 kpc), respectively.

The age profile of NGC 7217 presented in Fig. 1 exhibits specific features at the radii dominated by these three substructures. In the bulge-dominated region located mostly inside the nuclear star-forming ring (R = 10–12 arcsec), the mean stellar age decreases from 10 to 13 Gyr in the centre to 5 Gyr outwards. In the inner exponential component, the age stays nearly constant at about 5 Gyr; individual estimates at the radii between 20 and 50 arcsec have an rms of 0.7 Gyr in the major-axis profile and 0.9 Gyr in the minor-axis one. The outer exponential component (R = 60–110 arcsec) has an intermediate age of about 2–3 Gyr, whereas in the broad outer star-forming ring (R = 70–80 arcsec), it drops down to 1 Gyr. Surprisingly, at these radii, we also see a drop in the SSP-equivalent stellar metallicity down to −0.65 dex prominent in the eastern side of the galaxy but hardly detected in the western side, which is probably connected to the morphology and location of individual star-forming regions crossed by the slit. The mean metallicity of the bulge is close to the solar value, [Fe/H] = −0.06 dex, while the outer exponential component ([Fe/H] = −0.45 dex) is rather metal poor for such a massive galaxy. The inner exponential component

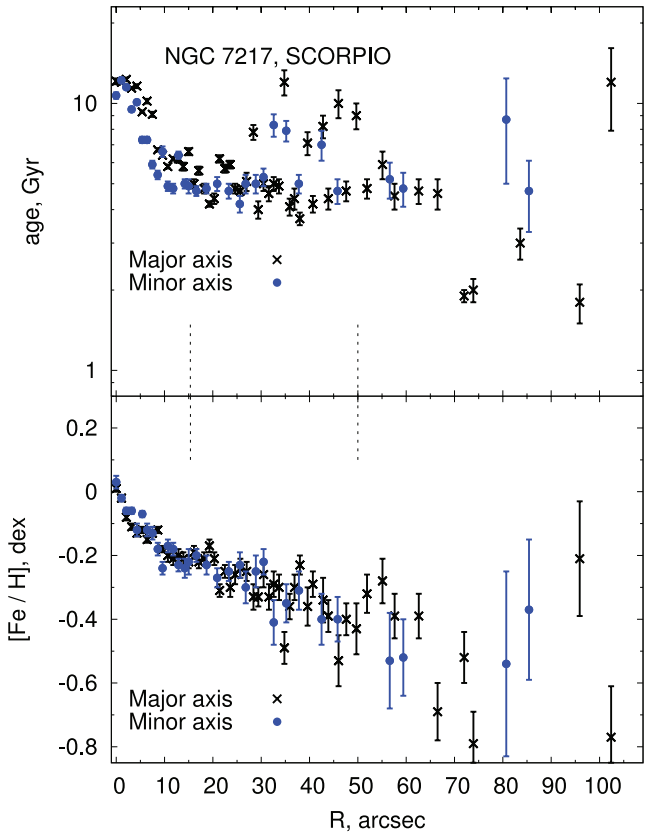

Figure 1. Radial distributions of the mean age (top panel) and metallicity (bottom panel) of the stellar populations measured along the major-axis (PA = 81°) and minor-axis (PA = 169°). The vertical dashed lines indicate the conventional boundaries of the bulge and the inner exponential component set at four scalelengths of each component.

has a mean metallicity of about −0.2 dex with a notable metallicity gradient around −0.3 dex per dex in radius.

Hence, the existence of the three components found in the photometric data by Sil'chenko & Afanasiev (2000), a bulge and two [probably] exponential discs, is supported by specific features in the stellar population profiles. Later, we will propose the evolutionary scenario of NGC 7217, where the two discs may have different origins.

We present the derived major-axis (PA = 81°) profiles of line-of-sight velocities for the gaseous and stellar components in Fig. 2. The Hβ emission-line component remains clearly visible along the whole extent of the galaxy where we can measure the stellar kinematics. [O III] is much weaker than Hβ at radii $R > 10$ arcsec. The velocities obtained from the two emission lines agree well, but those determined from Hβ in the outer region have four to five times smaller uncertainties. Therefore, we constructed the combined gaseous line-of-sight velocity profile displayed in Fig. 2 from [O III] and Hβ kinematics at radii below and above 10 arcsec, respectively. Both stellar and gaseous velocity profiles have similar shapes, including even some particular features such as a notable drop at $R \approx 50$ arcsec. They are also very symmetric. Therefore, for the dynamical analysis presented in the next section, we folded them along the galaxy centre and averaged the values of rotation velocities from both sides. The gaseous rotation velocities ($\sim$150 km s^{-1}) exceed the stellar ones ($\sim$120 km s^{-1}) by nearly 30 km s^{-1} at all radii, which is an observational manifestation of the asymmetric drift. The difference stays nearly constant between 10

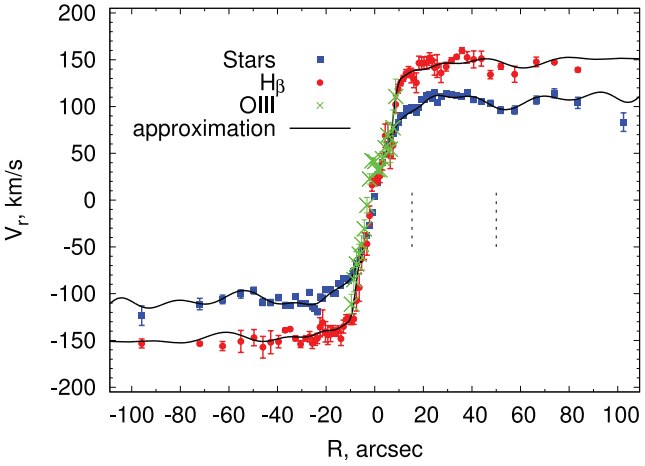

Figure 2. Radial distribution of the line-of-sight velocities of stars and the ionized gas along the major-axis (PA = 81°). The [O III] data are presented only for $|R| < 10$ arcsec. The vertical dashed lines indicate the conventional boundaries of the bulge and the inner exponential component (see Fig. 1).

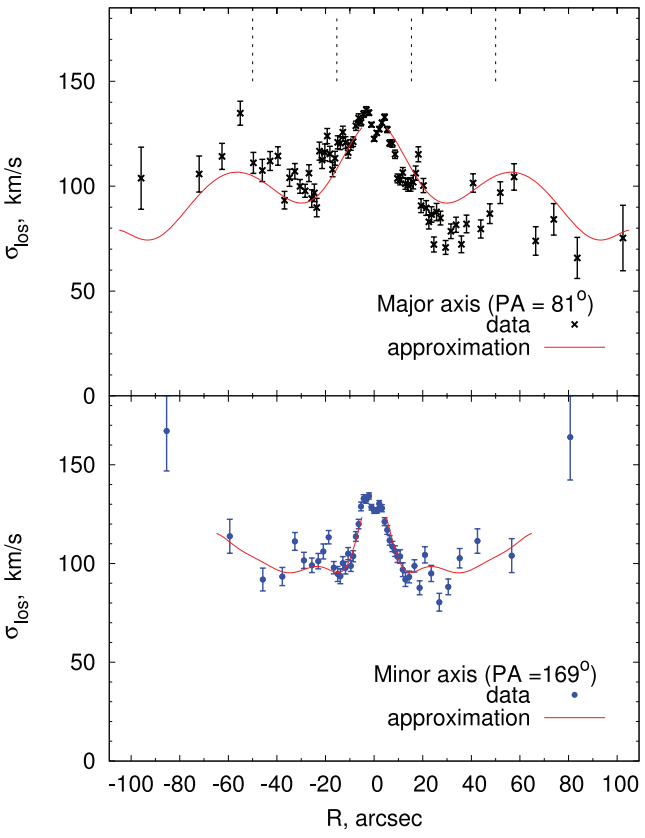

Figure 3. Radial distributions of the line-of-sight stellar velocity dispersion measured along the major-axis, PA = 81° (top panel) and minor-axis, PA = 169° (bottom panel). The vertical dashed lines indicate the conventional boundaries of the bulge and the inner exponential component (see Fig. 1).

and 70 arcsec, suggesting a similar dynamical status of the inner and outer exponential stellar structures. These structures are probably discs, but a quite high asymmetric drift implies that they should be rather thick.

In Fig. 3, we show the observed radial distributions of the line-of-sight stellar velocity dispersion along the minor-axis and major-axis of NGC 7217. Since the galaxy is seen nearly face-on, the

vertical (σ_z) component of the disc velocity ellipsoid creates the main contribution to the observed velocity dispersion. However, there is a notable difference between major-axis and minor-axis velocity dispersion profiles, suggesting significant contributions of the tangential (σ_φ) and radial (σ_R) velocity dispersions to the values along the major-axis and minor-axis, respectively. The main feature of the stellar line-of-sight velocity dispersion profiles of NGC 7217 is a minimum in the area of the inner exponential component and a smooth raise outwards. This behaviour is quite unexpected: as we demonstrated, the outer stellar component is younger than the inner one, so it would be more natural if the stellar subsystem formed recently from the dynamically cold gas is itself dynamically cold. However, the velocity dispersion rises beyond $R \approx 50$ arcsec is statistically significant and seen in both minor-axis and major-axis velocity dispersion profiles. In Section 5, we will give the possible explanation of these features.

4 DYNAMICAL ANALYSIS: TWO VERY DIFFERENT DISCS IN NGC 7217

We used our kinematical data to recover the stellar velocity ellipsoid and reconstruct the radial distributions of all stellar velocity dispersion components. Then, we calculated the stellar disc thickness profile from the σ_z radial distribution. By using relations describing the disc equilibrium, we did it independently from the major-axis and minor-axis kinematical data.

For an intermediately inclined galaxy, the two in-plane components of the stellar velocity dispersion, σ_R and σ_φ, are related to the observed minor-axis and major-axis line-of-sight velocity dispersions according to the following relations:

$$\sigma^2_{\rm los,min}(R\cos i) = \sigma^2_R \sin^2 i + \sigma^2_z \cos^2 i\,,$$
$$\sigma^2_{\rm los,maj}(R) = \sigma^2_\varphi \sin^2 i + \sigma^2_z \cos^2 i\,. \quad (2)$$

They also include the contribution from the vertical component of the velocity ellipsoid σ_z. Thus, by measuring the variations in the line-of-sight dispersions along the principal axes, we can obtain only a linear combination of $\sigma_R(R), \sigma_\varphi(R)$ and $\sigma_z(R)$. Therefore, we need additional information in order to derive all three velocity dispersion components from these equations. To close the system of equations (2), we can use some dynamical relations, which are valid if the system is in equilibrium. One such relation connects the velocity dispersion components $\sigma_R(R)$ and $\sigma_\varphi(R)$ via the mean azimuthal velocity of stars (Binney & Tremaine 1987):

$$\frac{\sigma^2_\varphi}{\sigma^2_R} = \frac{1}{2}\left(1 + \frac{\partial \ln \bar{v}_\varphi}{\partial \ln R}\right)\,. \quad (3)$$

If the rotational velocities are unknown, we can use the local circular speed of gas $v_{\rm c}$ instead of $\bar{v}_\varphi$ in order to relate σ^2_R to σ^2_φ:

$$\frac{\sigma^2_\varphi}{\sigma^2_R} = \frac{1}{2}\left(1 + \frac{\partial \ln v_{\rm c}}{\partial \ln R}\right)\,. \quad (4)$$

This relation is true if most orbits in a disc are quasi-circular.

Adding any of these relations, equation (3) or equation (4), to the two presented above enables us to recover radial distributions of all three velocity dispersion components. For the first time this technique was applied to the data for NGC 488 by Gerssen, Kuijken & Merrifield (1997). However, this procedure creates very noisy output when applied directly to the data, because it includes the subtraction of the two quantities $\sigma^2_{\rm los,min}$ and $\sigma^2_{\rm los,maj}$ with very close values, as well as the numerical derivation of $\bar{v}_\varphi$ or $v_{\rm c}$. A possible solution is to parametrize the kinematical profiles and to find the best-fitting solution (see e.g. Gerssen et al. 1997, 2000; Shapiro, Gerssen & van der Marel 2003) which will, however, depend on the adopted parametrization. For this reason, we adopted the less-parametric approach as in Noordermeer et al. (2008). We approximated all kinematical profiles using polynomials and calculated all quantities including their derivatives analytically. But even then, the subtraction of the major-axis velocity dispersion profile from the minor-axis one results in an unreliable and ambiguous solution. To avoid this, we use the asymmetric drift equation. The deprojected major-axis gas rotation is a measure of the circular speed $v_{\rm c}$, while the deprojected major-axis stellar velocities allow us to determine the mean rotational motion $\bar{v}_\varphi$ related to the radial velocity dispersion σ_R. Therefore, we can obtain the σ_R profile using the major-axis velocity profiles for gas and stars and the asymmetric drift equation (Binney & Tremaine 1987):

$$v^2_{\rm c} - \bar{v}^2_\varphi = \sigma^2_R\left(\frac{\sigma^2_\varphi}{\sigma^2_R} - 1 - \frac{\partial \ln \Sigma}{\partial \ln R} - \frac{\partial \ln \sigma^2_R}{\partial \ln R}\right)\,, \quad (5)$$

where Σ is the stellar surface density. Provided that the stellar mass-to-light ratio stays nearly constant [$(M/L)_I = 1.86$ in solar units from the PEGASE.2 models, see Fioc & Rocca-Volmerange 1997), we can use the surface brightness instead of the surface density Σ in equation (5). We assume that the I-band photometric data trace the old stellar population whose internal kinematics we are studying. Because of the logarithmic derivative, the exact choice of M/L is not critical. The asymmetric drift equation can be used directly to obtain the radial velocity dispersion profile, provided that the ratio between σ^2_φ and σ^2_R is determined from equation (3) or equation (4). However, equation (5) requires the knowledge of the σ_R radial gradient. We assume that in the outer regions of the galaxy between 30 and 70 arcsec, σ_R may decline exponentially as $\propto \exp(-R/h_{\rm kin})$ and use the last term in the form $2R/h_{\rm kin}$, where $h_{\rm kin}$ is a free parameter.

The choice of a radial velocity dispersion profile exponentially declining with the radius is physically motivated. There is a conventional assumption that the disc thickness and the z-component of the velocity dispersion σ_z are connected via the vertical equilibrium condition for an isothermal layer (Spitzer 1942):

$$\sigma^2_z(R) = \pi\, G\, \Sigma(R)\, z_0\,, \quad (6)$$

where z_0 is the half-thickness of a homogeneous layer. For a mass-to-light ratio constant with the radius, constant z_0 and an exponential brightness profile it yields

$$\sigma^2_z(R) \propto \exp(-R/h)\,, \quad (7)$$

where h is the disc scalelength.

The disc heating theory suggests that the range in the velocity anisotropy σ_z/σ_R is about 0.4–0.8 (Jenkins & Binney 1990), which is consistent with observations. Gerssen et al. (1997, 2000) and Shapiro et al. (2003) modelled the data for several galaxies and estimated the values for the velocity anisotropy σ_z/σ_R between 0.5 and 0.7, similar to the solar neighbourhood (Dehnen & Binney 1998).

Since the ratio σ_z/σ_R is close to constant, equation (7) yields

$$\sigma_R \propto \exp(-R/2\,h)\,. \quad (8)$$

It implies that $h_{\rm kin} = 2\,h$. This approach does work for our Galaxy (Lewis & Freeman 1989) but in the case of NGC 7217 we did not fix the value of $h_{\rm kin}$ and estimated it iteratively by fitting the radial velocity dispersion profile with the exponential law and substituting the value of $h_{\rm kin}$ in the asymmetric drift equation. We needed this value to estimate only the last term in equation (5). The exact

value of this term may affect the final results but the effect is quite insignificant. We were changing the range of R used to fit σ_R by exponential law and did not note any difference between final results. Having derived the σ_R radial distribution from equation (5), we can then compute the radial profile of the vertical component of the velocity dispersion σ_z using one of equation (2). We choose to use both of them to control the reliability of our results.

Finally, we can obtain the thickness profile from equation (6) which is valid for an isothermal layer. The assumption about the constant velocity dispersion along the z-direction for discs is in agreement with the results of N-body simulations (see e.g. fig. 2 in Sotnikova & Rodionov 2006). However, one should keep in mind that equation (6) gives the upper limit for the disc thickness. If there is a massive dark halo, the disc thickness will be lower for the same value of σ_z.

In order to deproject the velocity profiles, we need to know the inclination of the rotation plane to the line of sight. NGC 7217 has a roundish appearance; however, quite high observed (i.e. projected) rotation velocities suggest that it is not seen completely face-on. The isophote ellipticity analysis assuming the infinitely thin stellar disc provided the disc inclination estimates in the range of $i = 26°$–$28°$ (Verdes-Montenegro et al. 1995; Sánchez-Portal et al. 2000; Noordermeer & van der Hulst 2007), whereas the kinematical analysis usually results in slightly higher values of $i = 30°$–$31°$ (see Buta et al. 1995; Noordermeer et al. 2005 for the H I map analysis and Sil'chenko & Moiseev 2006 for the stellar kinematics). Keeping in mind the possible considerable thickness of the stellar disc, we adopt the inclination value of $i = 30°$. Varying i between 26° and 35° changes the resulting disc thickness estimates by no more than 10 per cent.

We present the reconstructed radial distributions of σ_R and σ_z in Fig. 4. We estimated uncertainties using a bootstrapping method (Press et al. 1992). We computed σ_R and σ_z assuming that the errors of observational quantities used in the procedure are distributed according to the normal law and changing input data points according to these errors. We made several thousand realizations of the procedure, averaged resulting values and estimated the dispersion of all the simulations at each point.

The data in Fig. 4 suggest that the dynamically coolest subsystem of NGC 7217 as concerning the vertical velocity dispersion is

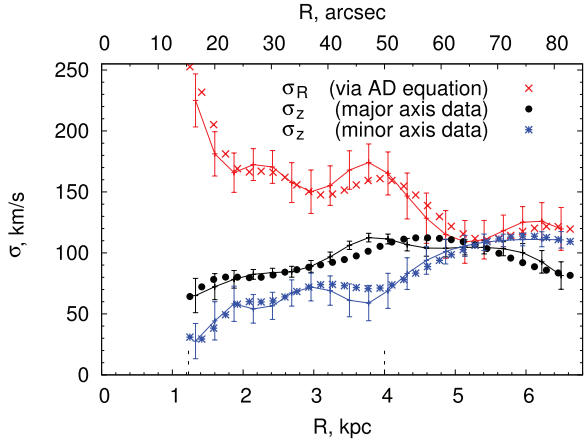

Figure 4. Radial distributions of the radial and vertical velocity dispersions reconstructed from the major-axis and minor-axis kinematical profiles. Full lines – profiles calculated via equation (3); symbols – profiles obtained by using equation (4). The error bars are shown only for profiles indicated by the solid lines. The vertical dashed lines indicate the conventional boundaries of the bulge and the inner exponential component (see Fig. 1).

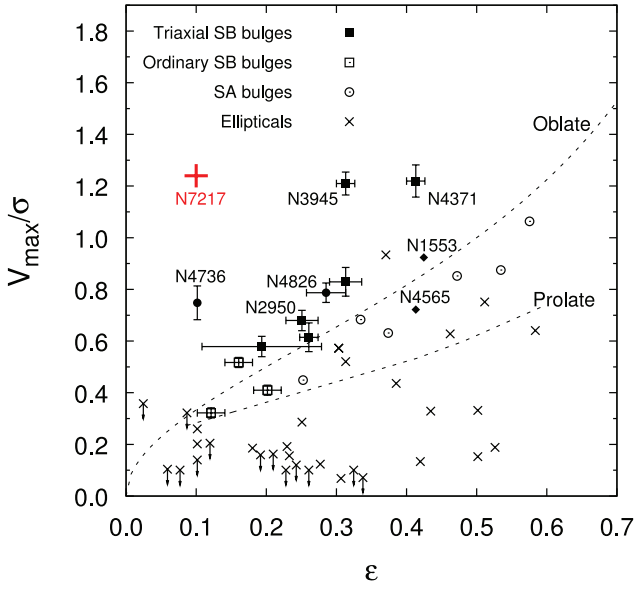

Figure 5. Relation between the ratios of observed maximal rotation velocities and velocity dispersions, and isophote ellipticities for early-type galaxies, bulges (open symbols) and pseudo-bulges (filled symbols). The models of prolate and oblate isotropic rotators are overplotted by the dashed lines. NGC 7217 is shown with a red cross being clearly above the locus of pseudo-bulges from Kormendy & Kennicutt (2004).

the *inner* stellar exponential component. Therefore, it is certainly a disc and not a pseudo-bulge. Indeed, in Fig. 5, we plot the inner exponential component of NGC 7217 in the diagram of Binney–Kormendy. With its $\epsilon \approx 0.1$ and $v_{\max}/\sigma_{\rm los} = 1.24$ it stays well above all the pseudo-bulges dynamically confirmed by Kormendy. At $R > 30$ arcsec (>2.4 kpc), the vertical velocity dispersion component slowly raises outwards reaching 110 km s^{-1} at the location of the outer star-forming ring. The σ_R profile decreases along the radius as expected, but in the transition region where the outer disc starts to dominate ($R = 40$–50 arcsec; 3.2–4.0 kpc), we see a break of the monotonic fall. The whole σ_R profile can be divided into two parts corresponding to the two exponential stellar components.

The disc 'thickness profiles' at radii $R = 15, \ldots, 80$ arcsec reconstructed from the major-axis and minor-axis kinematics are shown in Fig. 6. While the qualitative agreement between them exists, quantitatively, they diverge at some radii. As it was mentioned in Section 2, the minor-axis data are of a worse quality than the major-axis ones, but they are featureless as concerning the line-of-sight stellar velocity dispersion. Thus, both data sets have their shortcomings and neither of them can be preferred. One of the sources of the profile discrepancy might be the adopted inclination angle and the discrepancy between measured distances along the major-axis and deprojected distances along the minor-axis. Similarly to the σ_z profile behaviour, we see that the inner stellar disc is relatively thin ($z_0 = 0.2, \ldots, 0.7$ kpc). Hence, at its inner boundary, the ratio of its scalelength to the scaleheight is about 4–5. The outer disc flares vigorously, reaching the half-thickness of 2.5–3 kpc at the outer star-forming ring position.

5 DISCUSSION

5.1 Explaining the structure of NGC 7217

From the analysis of the stellar and gaseous kinematics (line-of-sight velocities and velocity dispersion radial distributions) over

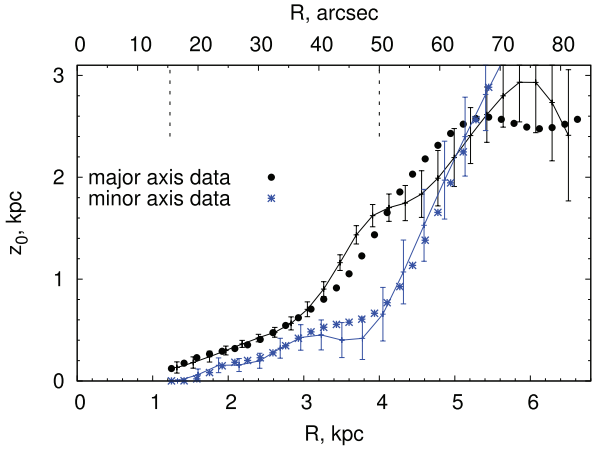

Figure 6. Radial distribution of the stellar disc scaleheight – the reconstructed 'edge-on' view. The solid lines are the profiles calculated via equation (3), while the symbols are for the profiles obtained by using equation (4). The error bars are shown only for profiles indicated by the solid lines. The vertical dashed lines indicate the conventional boundaries of the bulge and the inner exponential component (see Fig. 1).

an extended area of the giant early-type disc galaxy NGC 7217, we reconstructed the velocity ellipsoid and calculated the stellar disc scaleheights at radii from 20 to 70 arcsec (1.6–6 kpc). Earlier, Sil'chenko & Afanasiev (2000) demonstrated that this radial range contains two stellar substructures having exponential surface brightness profiles with different scalelengths, the inner one with relatively low h and the outer one with more extended (standard for giant galaxies) scalelength. Our analysis reveals that the inner component has the scaleheight of 0.2–0.7 kpc and the outer one has the scaleheight of about 1–3 kpc. Hence, we can classify the inner and outer components as thin and thick stellar discs, respectively.

Having applied the full spectral fitting NBURSTS technique with a grid of high-resolution SSP models, we deduced mean ages and metallicities of stars. The inner disc exhibits the intermediate age of about 5 Gyr and the mean metallicity of −0.2 dex with a strong negative metallicity gradient along the radius. The outer disc is quite metal-poor ([Fe/H] = −0.4 dex) and relatively young (2 Gyr). The outer disc harbours a prominent star-forming ring with the mean age of about 1 Gyr at the radius of $R \approx 75$ arcsec very well visible in ultraviolet data from the *GALEX* satellite and 8-m near-infrared data from the *Spitzer Space Telescope*. Interestingly, in this ring, the mean stellar metallicity falls down to a very low value of −0.7 dex. The galaxy nucleus and the bulge of NGC 7217 inside the nuclear star-forming ring are very old (∼13–15 Gyr).

How can we explain the complex structure of NGC 7217? In principle, the fact that the outer stellar disc is younger than the inner one is in line with the paradigm of the 'inside-out' disc formation. However, the sharp boundary between the two discs where the properties, including the stellar age and metallicity, as well as the radial and vertical scalelengths of the star distribution, change abruptly hints to a temporal gap between the inner and outer disc formation or to some catastrophic event that provoked the expansion of star formation into the outer ring area.

Interestingly, the molecular gas concentrates in the inner disc (Combes et al. 2004), while the neutral hydrogen is observed in the narrow ring in the outer disc (Buta et al. 1995; Verdes-Montenegro et al. 1995; Noordermeer et al. 2005). However, star formation is almost absent in the inner disc (though it burns in the nuclear star-forming ring between the bulge and the inner disc) and is very prominent in the outer disc (Battinelli et al. 2000). Noordermeer et al. (2005) estimated the gravitational stability of the gas in the outer ring and the threshold density for star formation according to the Kennicutt (1989) criterion:

$$\Sigma_{\rm cr} = \alpha \frac{\kappa c}{3.36G}, \tag{9}$$

where κ is the epicyclic frequency that can be derived from the rotation and c is the gas velocity dispersion, which can be assumed as a constant value of 6 km s^{-1}. For the dimensionless quantity α, Kennicutt derived a value of 0.67 from the empirical study of star formation cut-offs in spiral galaxies. Dynamically, it means that one should take into account non-axisymmetric modes while considering the stability of a disc, because for axisymmetric modes $\alpha = 1$ (Toomre 1964). Noordermeer et al. (2005) demonstrated that even in the middle of the H I ring of NGC 7217, the gas density does not exceed 25 per cent of the critical one. The estimate by Noordermeer et al. (2005) did not take into account the existence of a stellar disc. Having restored the velocity dispersion profile σ_R for stars, we can evaluate the gaseous disc stability in the framework of the two-fluid approach (Jog & Solomon 1984; Efstathiou 2000):

$$\Sigma_{\rm cr} = \frac{\kappa c}{3.36Gg(a,b)}, \tag{10}$$

where a and b are the ratios of the stellar to gas velocity dispersion and surface densities, respectively, and $g(a, b)$ is a function derived numerically by Efstathiou (2000). This approach results in the critical density estimate at least twice lower than the value obtained by Noordermeer et al. (2005). However, even then the critical density remains too high (see Fig. 7). Therefore, the gas in the outer ring must be gravitationally stable and why the star formation proceeds there is still an open question. The very existence of a system of star-forming, gas-populated rings in an unbarred galaxy is a puzzle. Combes et al. 2004 discussed a possibility of a past bar, strong or weak, which had formed the rings and then had dissolved after the gas inflow had supplied mass into the centre. Now we see that this scenario experiences strong difficulties: the stellar population in the NGC 7217 centre is very old and it is clear that no significant star formation took place there for the last 5 Gyr in order to provide mass concentration and subsequent bar destruction.

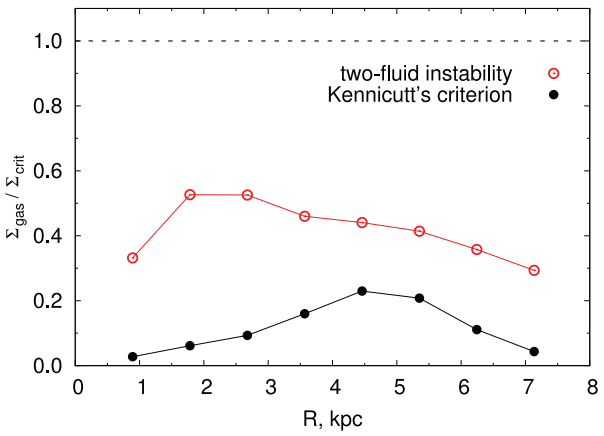

Figure 7. Ratio between the observed gas density and critical density according to Kennicutt (1989) and the two-fluid instability (Jog & Solomon 1984; Efstathiou 2000) criteria. The dashed line indicates the threshold for star formation. The H I surface density profile was taken from Noordermeer et al. (2005).

5.2 Inner polar disc

In Fig. 8, we present the minor-axis kinematics and emission-line properties in the central region of NGC 7217 derived from the analysis of the stellar population spectral fitting residuals. In the nuclear region, the [N I] doublet is clearly detected in addition to the oxygen and hydrogen lines. The [O III] kinematics are evidence of either a rotating disc or an outflow from the galaxy centre which can be induced by an active nucleus. We measured the emission-line ratios (see the bottom panel in Fig. 8) and used the ITERA tool (Groves & Allen 2010) providing a large collection of emission-line models for different excitation mechanisms to perform the diagnostics. The extremely high $\log([\mathrm{N\,I}]/\mathrm{H}\beta) > 0$ ratio, given moderate $\log([\mathrm{O\,III}]/\mathrm{H}\beta) \approx 0.45$, is consistent with either a shock ionization for solar or subsolar metallicities of the interstellar medium or an AGN having a significantly supersolar metallicity (e.g. $>+0.3$ dex). Given very moderate metallicity of the stellar population in the central region of NGC 7217, the latter possibility can be ruled out at a high level of confidence. Therefore, we are probably observing an inner polar disc in NGC 7217, which is supported by the direct inspection of the *Hubble Space Telescope* (*HST*) imaging data in the narrow Hα + [N II]λ6583 centred filter (Fig. 9).

According to Karachentseva (1973), NGC 7217 is an isolated galaxy, not a member of any group, and its environment is empty

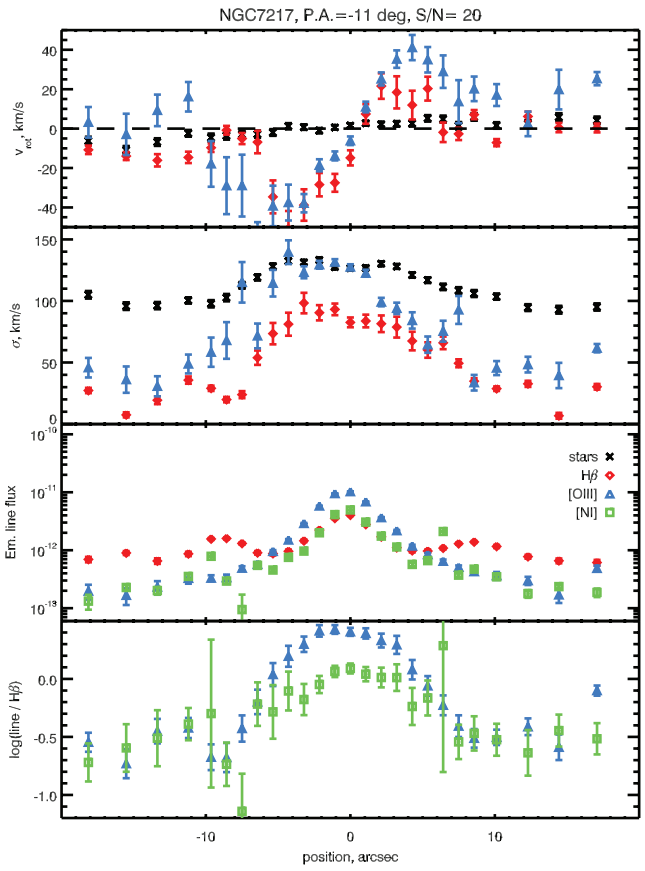

Figure 8. Minor-axis kinematics and emission-line properties of NGC 7217 from the analysis of the Hβ (red, diamonds), [O III] (λ = 5007 Å, blue, triangles), and [N I] (λ = 5197/5200 Å, green, squares) lines in its spectra with the best-fitting stellar population models subtracted. The panels show (from the top to bottom): radial velocities, velocity dispersion, line fluxes and logarithms of the emission-line ratios: [O III]/Hβ (blue) and [N I]/Hβ (green).

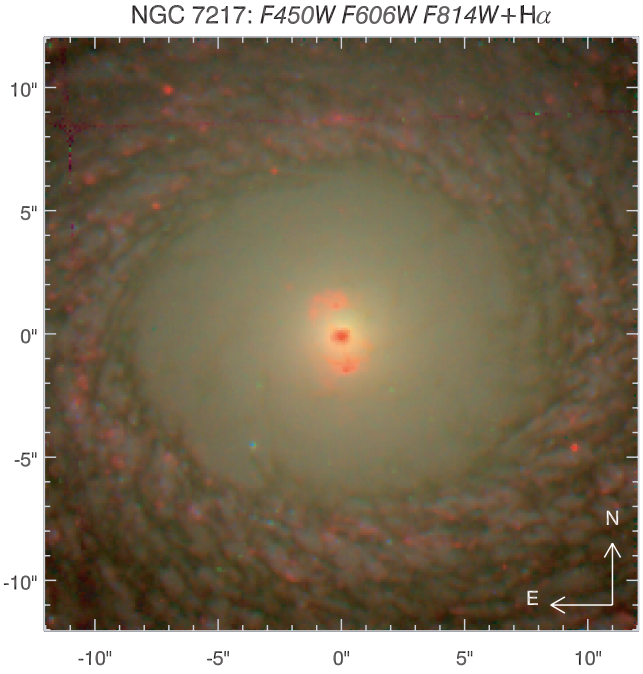

Figure 9. Inner polar disc in NGC 7217 as seen with the *HST*. This false colour composite is made of *F*450*W*, *F*606*W* and *F*814*W* WFPC2 images with the Hα fluxes from the ACS *F*658*N* images added to the red channel using the Lupton et al. (2004) algorithm. The strongly inclined gaseous structure seen here in the centre is a polar disc, because the outer disc is seen almost face-on with its major-axis nearly horizontal in this plot.

of satellites. However, Merrifield & Kuijken (1994) and Sil'chenko & Afanasiev (2000) suggested the presence of a counter-rotating stellar component in the central region of NGC 7217; moreover, we see also the inner polar gaseous disc. Hence, accretion or minor merger(s) in the past seem inevitable. If we assume that the galaxy centre is its oldest part, then we can suspect the vertical impact by a gas-rich satellite. Then, the 0.3-kpc nuclear polar disc in NGC 7217 is a remnant of the satellite gaseous component which conserved its initial orbital momentum. The close analogue of such an event is the Sagittarius dSph disruption by the Galaxy accompanied by the redistribution of the satellite material along the polar large circle. Polar orbits are known to be stable; hence, this gas cannot accrete to the very centre, explaining why the fuel for the star formation in the centre of NGC 7217 has been absent, until now evidenced by the old stellar population there.

Such a vertical impact is also able to produce a system of star-forming/stellar rings by exciting a running compression wave in a large-scale galaxy disc (Athanassoula, Puerari & Bosma 1997). Moreover, the simulations of a Cartwheel-like galaxy by Mapelli et al. (2008) for 1.5 Gyr after the impact clearly show that sharp stellar rings formed initially expand over a large area during 1 Gyr and form a structure resembling a low surface brightness outer stellar disc. The two-tiered exponential stellar disc of NGC 7217 could have been built by such a minor merger. However, we still need a triaxiality of the potential in order to produce a counter-rotating component in the inner disc during the same event: the polar gas in the tumbling triaxial potential has to warp in the outer part in such a sense that it arrives to the rotational plane of stars with the opposite spin (van Albada, Kotanyi & Schwarzschild 1982). Being compressed, this gas would be consumed by star formation, leaving a counter-rotating stellar component. Besides, the triaxial potential also creates long-living resonance rings in contrast to short-living

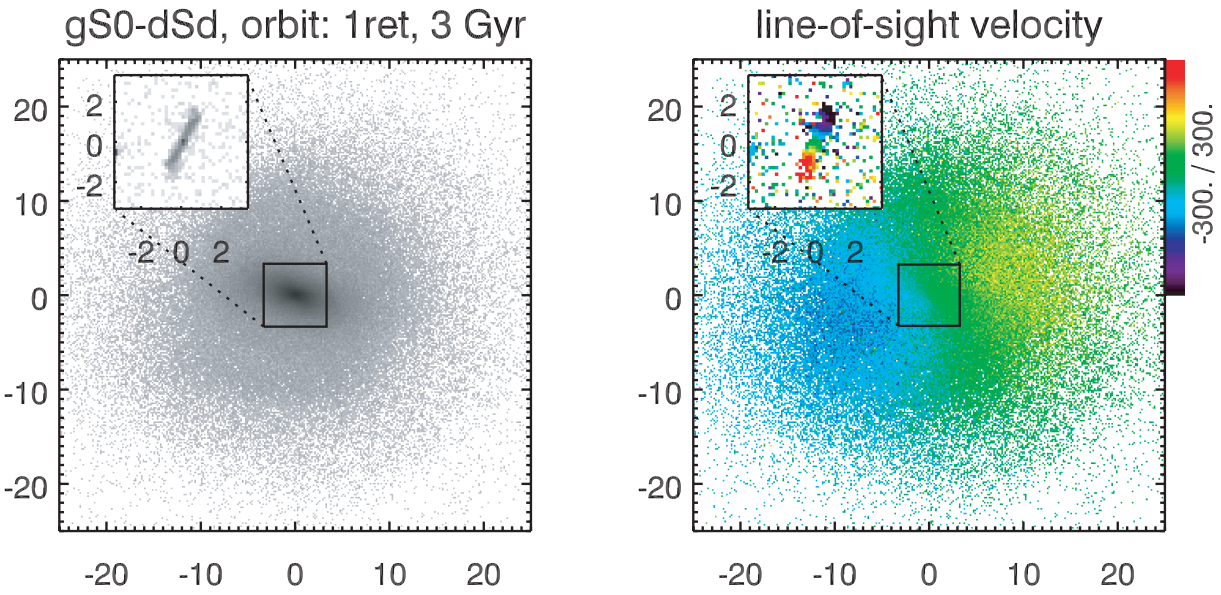

Figure 10. Left-hand panel: surface density of stars and the gas (inset) for a minor wet merger of gS0 and dSd galaxies (mass ratio 10:1) on a retrograde orbit. Right-hand panel: line-of-sight velocities of stars and the gas (inset) for the same merger. The signature of the inner polar ring seen edge-on is clearly visible. The orientation of the galaxy disc is chosen to match that of NGC 7217 ($i = 30^\circ$). The axes are in kpc.

collisional rings. From our data we cannot distinguish between a triaxial dark matter halo and a low-contrast extended stellar spheroid (see discussion in Buta et al. 1995).

5.3 Insights from simulations

Simulations of vertical impacts producing ring structures reveal that the vertical oscillations of disc stars excited by the intruder's passage result in strong thickening of the stellar disc (Hernquist & Weil 1993) which we probably observe in the outer disc of NGC 7217. The small thickness of the inner disc can be perhaps explained by its high density, increased after the impact by the counter-rotating component and also by the presence of significant molecular gas content (Combes et al. 2004). Interestingly, in the recognized vertical collision product, the famous Cartwheel galaxy, the molecular gas concentrates in the central region, while the neutral atomic hydrogen is confined to the outer ring (Horellou et al. 1998) being very similar to NGC 7217.

One can suggest another explanation of the inner disc structure. It could have been formed from the material of a small satellite during its complete disruption (Eliche-Moral et al. 2006). This new inner disc can be older than the outer one because the infalling stars were initially older. It can also be dynamically cold because its material had experienced the orbital circularization. However, this scenario requires a nearly in-plane encounter. The unusually high thickness of the outer component and the presence of the inner polar disc in NGC 7217 make us to prefer encounters at higher inclinations.

The minor-merger scenario with a vertical impact requires this event to have occurred long time ago. The galaxy needs time to convert the counter-rotating gas into stars and to establish the mean stellar age of 5 Gyr in the compact high-density inner stellar disc. Then, the current star formation in the outer disc involving very low-metallicity gas does not relate to this event and to its collision rings. It may be provoked by the later gas infall in a tidal tail developed during the minor merger. This mechanism can explain the patchy and filamentary edges of the H I ring in the map of NGC 7217 (Noordermeer et al. 2005) and the presence of the shock-induced star formation in the low-density gas ring which had to be gravitationally stable under the quiescent conditions.

We explored intermediate-resolution (0.2 kpc) TreeSPH simulations of minor mergers provided by the GalMer data base[3] (Chilingarian et al. 2010). Presently, available simulations include interactions of a gas-free giant lenticular galaxy ('gS0') with a 10 times less-massive dwarf galaxy. The morphology of a dwarf spans the entire Hubble sequence from non-rotating ellipticals ('dE0') to bulgeless discs ('dSd'). Here we consider only gS0–dSd mergers, as this configuration has the largest quantity of gas compared to other morphologies of a satellite galaxy. The inclination of the orbital plane to the rotation planes of the two interacting galaxies is 33° for a giant S0 and 130° for dSd. The two sets of numerical experiments include interactions on prograde and retrograde orbits with different initial orbital momenta and motion energies (24 in total). The simulations were run for a total duration of 3 Gyr.

The bar is always formed in the gS0 stellar disc. Merger remnant morphologies vary quite a lot, but all of them can be classified into two families related to the mutual orientation of the infalling satellite internal angular momentum with respect to that of the orbital motion.

All retrograde encounters result in the formation of a strongly inclined inner star-forming ring in the gS0 galaxy having a radius of ≈1 kpc. Its plane is orthogonal to the initial orbital plane of an interaction, that is, its inclination to the gS0 disc plane is about 60°. This ring is located in the inner bright part of the S0 bulge and its contribution to the total stellar light (and, consequently, to the stellar kinematics derived from the spectra) in the central region of the galaxy is negligible (see the left-hand panel of Fig. 10). However, it is immediately revealed by the gas kinematics (see the right-hand panel of Fig. 10), as it is the only structure with significant gas content. Although the mass ratio of 1:10 in the *total mass* is quite high, none of the retrograde encounters heated up significantly the large-scale S0 disc.

[3] http://galmer.obspm.fr/

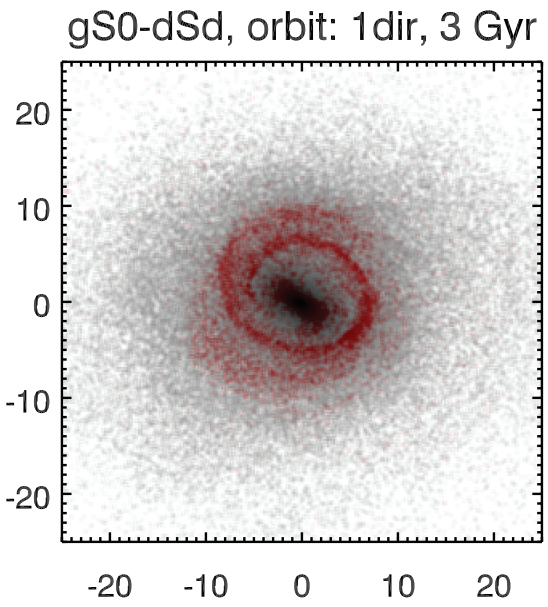

Figure 11. Surface density of stars (grey-scale) and the gas (red) for a minor wet merger of gS0 and dSd galaxies (mass ratio 10:1) on a prograde (direct) orbit. The orientation of the galaxy disc is chosen to match that of NGC 7217 ($i = 30^\circ$). The axes are in kpc.

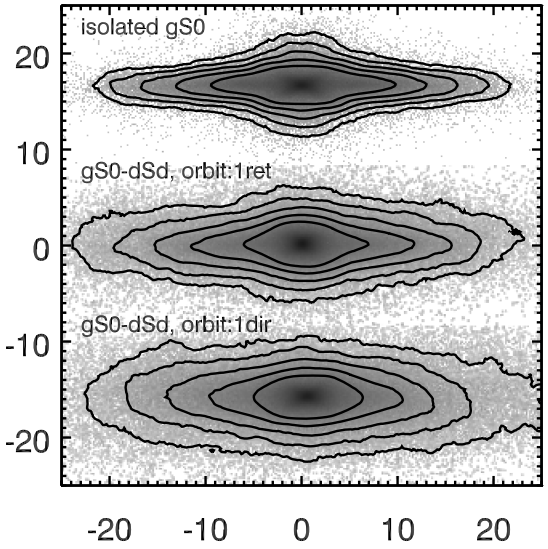

Figure 12. Disc thickening by minor mergers. The edge-on view of the GalMer model of a giant S0 galaxy in isolation is shown in the top and the remnants of minor mergers with a gas-rich dSd galaxy (mass ratio 10:1, orbit type 1, see text) on retrograde and prograde orbits are displayed in the middle and bottom, respectively. The contours are separated by 1 mag arcsec^{-2}; the axes are in kpc.

The situation is totally different for prograde encounters. They heat and thicken the gS0 disc significantly, nearly destroying it for certain orbital types with high motion energies. The gas and newly formed stars from the infalling satellite form a large-scale corotating disc in the main plane of the gS0 galaxy or between its initial plane orientation and the orbital plane if the large-scale stellar disc is destroyed. If the large disc survives, the gas settles at its plane being concentrated at one of its resonances, probably the outer bar resonance, creating a star-forming ring having $R \approx 8$ kpc quite thick ($\sim$1 kpc) in the radial direction (see Fig. 11). As it resides in a region where the surface density of the gS0 disc is rather low, it creates significant contribution to the galaxy light. Since the initial metallicity of the interstellar medium in dSd is low, the newly formed stars in this ring will also have low metallicities being in agreement with young metal-poor stars detected by our stellar population analysis in the outer ring of NGC 7217. Worth mentioning that due to the intense heating, the large-scale gS0 disc flares in the outer regions of a galaxy (see Fig. 12). The outer disc must have formed by this event not very long time ago; otherwise, we would have expected to see young metal-poor stars formed in it migrating inwards and erasing an observed quite sharp break in the age profile. The characteristic migration time of about 1 Gyr in a Milky Way like galaxy using the mechanism proposed recently by Minchev & Famaey (2010) and Minchev et al. (2011) allows us to constrain the formation epoch of the outer disc of NGC 7217.

Hence, we conclude that the scenario of two consequent minor mergers at different orbits provides a plausible explanation to the observed structure of NGC 7217.

6 SUMMARY

We performed the analysis of internal kinematics and stellar population properties in the nearby isolated early-type disc galaxy NGC 7217 having star-forming rings by the NBursts full spectral fitting of deep long-slit intermediate-resolution spectroscopic data.

The age and metallicity profiles of NGC 7217 exhibit three components that well correspond to those found in the structural analysis of the galaxy by Sil'chenko & Afanasiev (2000): an old metal-rich bulge dominating at radii 0.4–1.2 kpc, the inner disc with the mean age of 5 Gyr and slightly subsolar metallicity at 1.6–4 kpc, and the outer metal-poor relatively young disc ($t = 2$–3 Gyr) beyond 4.8 kpc.

We analysed the parametrized major-axis and minor-axis kinematical profiles of NGC 7217, recovered the velocity ellipsoid in the regions dominated by the exponential discs and obtained the scaleheight radial profile. We concluded that the inner disc is thin ($z_0 = 0.2, \ldots, 0.7$ kpc), while the outer disc flares reaching the half-thickness of 2.5 kpc in the region of the outer star-forming ring. Using the two-fluid approach, we evaluated the gaseous disc stability in NGC 7217 and showed that even the highest density neutral-hydrogen ring at $R = 6$ kpc should be stable.

From the analysis of emission-line ratios in the residuals of the spectral fitting of NGC 7217, we ruled out a strong nuclear activity as the mechanism of circumnuclear gas excitation and concluded that the peculiar ionized-gas kinematics in the central region of NGC 7217 was due to the presence of the inner polar disc.

By comparing our data with the numerical simulations of wet minor mergers in the GalMer data base, we explained the observed structure and kinematics of NGC 7217 by the two consequent minor mergers with satellites having different initial orbits. The encounter on a retrograde orbit resulted in the formation of the inner polar disc, while the outer star-forming ring and the outer disc thickening were consistent with a minor merger on a prograde orbit.

ACKNOWLEDGMENTS

We thank Alexei Moiseev for the useful discussions. We are indebted to Alister Graham for his consultation. We are also grateful to our anonymous referee whose suggestions helped us to improve the clarity and presentation of the results. This research is partly based on observations made with the NASA/ESA *HST*, obtained

from the data archive at the Space Telescope Science Institute, which is operated by the Association of Universities for Research in Astronomy, Inc., under NASA contract NAS 5-26555. The work on the study of young stellar rings in disc galaxies is supported by the grants of the Russian Foundation for Basic Researches number 10-02-00062a and number 09-02-00968a.

REFERENCES

Afanasiev V. L., Moiseev A. V., 2005, Astron. Lett., 31, 194
Andredakis Y. C., Sanders R. H., 1994, MNRAS, 267, 283
Andredakis Y. C., Peletier R. F., Balcells M., 1995, MNRAS, 275, 874
Athanassoula E., Puerari I., Bosma A., 1997, MNRAS, 286, 284
Balcells M., Graham A. W., Domínguez-Palmero L., Peletier R. F., 2003, ApJ, 582, L79
Balcells M., Graham A. W., Peletier R. F., 2007, ApJ, 665, 1084
Battinelli P., Capuzzo-Dolcetta R., Hodge P. W., Vicari A., Wyder T. K., 2000, A&A, 357, 437
Bettoni D., Galletta G., Prada F., 2001, A&A, 374, 83
Binney J., Tremaine S., 1987, Galactic Dynamics. Princeton Univ. Press, Princeton, NJ
Buta R., Crocker D. A., 1993, AJ, 105, 1344
Buta R., van Driel W., Braine J., Combes F., Wakamatsu K., Sofue Y., Tomita A., 1995, ApJ, 450, 593
Cappellari M., Emsellem E., 2004, PASP, 116, 138
Chilingarian I. V., 2009, MNRAS, 394, 1229
Chilingarian I., Prugniel P., Sil'chenko O., Koleva M., 2007a, in Vazdekis A., Peletier R. R., eds, Proc. IAU Symp. 241, Stellar Populations as Building Blocks of Galaxies. Cambridge Univ. Press, Cambridge, p. 175
Chilingarian I. V., Prugniel P., Sil'chenko O. K., Afanasiev V. L., 2007b, MNRAS, 376, 1033
Chilingarian I. V., Cayatte V., Durret F., Adami C., Balkowski C., Chemin L., Laganá T. F., Prugniel P., 2008, A&A, 486, 85
Chilingarian I. V., Novikova A. P., Cayatte V., Combes F., Di Matteo P., Zasov A. V., 2009, A&A, 504, 389
Chilingarian I. V., Di Matteo P., Combes F., Melchior A., Semelin B., 2010, A&A, 518, A61
Combes F., Sanders R. H., 1981, A&A, 96, 164
Combes F. et al., 2004, A&A, 414, 857
Dehnen W., Binney J. J., 1998, MNRAS, 298, 387
Drory N., Fisher D. B., 2007, ApJ, 664, 640
Efstathiou G., 2000, MNRAS, 317, 697
Eliche-Moral M. C., Balcells M., Aguerri J. A. L., González-García A. C., 2006, A&A, 457, 91
Erwin P., Sparke L. S., 2002, AJ, 124, 65
Erwin P., Beltrán J. C. V., Graham A. W., Beckman J. E., 2003, ApJ, 597, 929
Fioc M., Rocca-Volmerange B., 1997, A&A, 326, 950
Freeman K. C., 1970, ApJ, 160, 811
Friedli D., Benz W., 1995, A&A, 301, 649
Gerssen J., Kuijken K., Merrifield M. R., 1997, MNRAS, 288, 618
Gerssen J., Kuijken K., Merrifield M. R., 2000, MNRAS, 317, 545
Graham A. W., 2001, AJ, 121, 820
Groves B. A., Allen M. G., 2010, New Astron., 15, 614
Hernquist L., Weil M. L., 1993, MNRAS, 261, 804
Horellou C., Charmandaris V., Combes F., Appleton P. N., Casoli F., Mirabel I. F., 1998, A&A, 340, L51
Ibata R., Mouhcine M., Rejkuba M., 2009, MNRAS, 395, 126
Jenkins A., Binney J., 1990, MNRAS, 245, 305
Jog C. J., Solomon P. M., 1984, ApJ, 276, 114
Karachentseva V. E., 1973, Soobshch. Spets. Astrofiz. Obs., 8, 3
Kennicutt R. C., Jr, 1989, ApJ, 344, 685
Kormendy J., 1993, in Dejonghe H., Habing H. J., eds, Proc. IAU Symp. 153, Galactic Bulges. Kluwer, Dordrecht, p. 209
Kormendy J., Kennicutt R. C., Jr, 2004, ARA&A, 42, 603
Laurikainen E., Salo H., Buta R., 2005, MNRAS, 362, 1319
Le Borgne D., Rocca-Volmerange B., Prugniel P., Lançon A., Fioc M., Soubiran C., 2004, A&A, 425, 881
Lewis J. R., Freeman K. C., 1989, AJ, 97, 139
Lupton R., Blanton M. R., Fekete G., Hogg D. W., O'Mullane W., Szalay A., Wherry N., 2004, PASP, 116, 133
Mapelli M., Moore B., Ripamonti E., Mayer L., Colpi M., Giordano L., 2008, MNRAS, 383, 1223
Merrifield M. R., Kuijken K., 1994, ApJ, 432, 575
Minchev I., Famaey B., 2010, ApJ, 722, 112
Minchev I., Famaey B., Combes F., Di Matteo P., Mouhcine M., Wozniak H., 2011, A&A, 527, A147
Moiseev A. V., 2008, Astrophys. Bull., 63, 70
Mollenhoff C., Heidt J., 2001, A&A, 368, 16
Noordermeer E., van der Hulst J. M., 2007, MNRAS, 376, 1480
Noordermeer E., van der Hulst J. M., Sancisi R., Swaters R. A., van Albada T. S., 2005, A&A, 442, 137
Noordermeer E., Merrifield M. R., Aragón-Salamanca A., 2008, MNRAS, 388, 1381
Pohlen M., Trujillo I., 2006, A&A, 454, 759
Press W. H., Teukolsky S. A., Vetterling W. T., Flannery B. P., 1992, Numerical Recipes in C: The Art of Scientific Computing. Cambridge Univ. Press, Cambridge, p. 691
Russell D. G., 2002, ApJ, 565, 681
Salpeter E. E., 1955, ApJ, 121, 161
Sánchez-Portal M., Díaz Á. I., Terlevich R., Terlevich E., Álvarez Álvarez M., Aretxaga I., 2000, MNRAS, 312, 2
Seigar M. S., James P. A., 1998, MNRAS, 299, 672
Shapiro K. L., Gerssen J., van der Marel R. P., 2003, AJ, 126, 2707
Sil'chenko O. K., Afanasiev V. L., 2000, A&A, 364, 479
Sil'chenko O. K., Moiseev A. V., 2006, AJ, 131, 1336
Sotnikova N. Y., Rodionov S. A., 2006, Astron. Lett., 32, 649
Spitzer L., Jr, 1942, ApJ, 95, 329
Toomre A., 1964, ApJ, 139, 1217
van Albada T. S., Kotanyi C. G., Schwarzschild M., 1982, MNRAS, 198, 303
van der Marel R. P., Franx M., 1993, ApJ, 407, 525
van Dokkum P. G., 2001, PASP, 113, 1420
Verdes-Montenegro L., Bosma A., Athanassoula E., 1995, A&A, 300, 65

This paper has been typeset from a TEX/LATEX file prepared by the author.